Electronic Supplementary Material (ESI) for New Journal of Chemistry.

Rationally Designed Tröger's base Decorated Bis-carbazoles as Twisted Solid-State Emitting Materials and Dead Bacterial Cell Imaging

Valmik P. Jejurkar,[a] Gauravi Yashwantrao,[a] Atharva Suryavanshi,[b] Nishigandha Mone,[c] Vaibhav Madiwal,[d] Anuja P. Ware,[e] Subhas S. Pingale,[e] Surekha Satpute,[c] Jyutika Rajwade,[d] and Satyajit Saha*[a]

[a]Department of Speciality Chemicals Technology, Institute of Chemical Technology (ICT), Mumbai-400019, India
[b]Dept. of Chemical Engineering, ICT Mumbai
[c]Dept. of Microbiology, Savitribai Phule Pune University (SPPU), Pune, India
[d] Nanobioscience Group, Agharkar Research Institute, Pune, India
[e]Dept. of Chemistry, SPPU, Pune

Table of Contents

General Aspects: All chemicals were purchased from available commercial sources like Sigma-Aldrich, Spectrochem, and Avra and used without further purification. Organic solvents were dried and distilled before the use. Silica gel-coated aluminium sheets (ACME, 254F) were used for the Thin Layer Chromatography (TLC) analysis using EtOAc and petroleum ether as the eluents. Melting points reported were uncorrected and were recorded using a capillary melting point apparatus (Thomas Hoover). Fourier transform infrared (FTIR) spectra were obtained with a Shimadzu spectrophotometer (FT-IR-8300). The ^{1}H nuclear magnetic resonance (^{1}H NMR) spectroscopy was carried out at 400 MHz on a Bruker 400 and 500 MHz spectrometer using $CDCl_3$ and dimethyl sulfoxide-d_6 (DMSO-d_6) as a solvent. Chemical shifts are reported in parts per million (ppm) downfield from TMS, and the spin multiplicities are described as s (singlet), d (doublet), t (triplet), dd (doublet of doublets), brs (broad singlet), and bd (broad doublet). Coupling constant (J) values are reported in hertz (Hz). Thermogravimetric analysis (TGA) was conducted on a Perkin-Elmer Diamond TG/DTA instrument at a heating rate of 10 °C/min under a nitrogen atmosphere with a flow rate of 50 mL/min. UV-Visible absorption spectra were obtained on a Perkin lambda 950 spectrophotometer. Cyclic voltammetry (CV) measurements were measured in an electrolyte solution of tetrabutylammonium perchlorate (*n*-Bu_4NClO_4) in acetonitrile (0.1 M) under an argon atmosphere, using platinum gauze and Ag/AgCl as the counter and reference electrodes, respectively. A scan rate of 50 mV/s was used during the CV measurements.

Fluorescence spectra of 4a, 4b, and 4c in different solvents

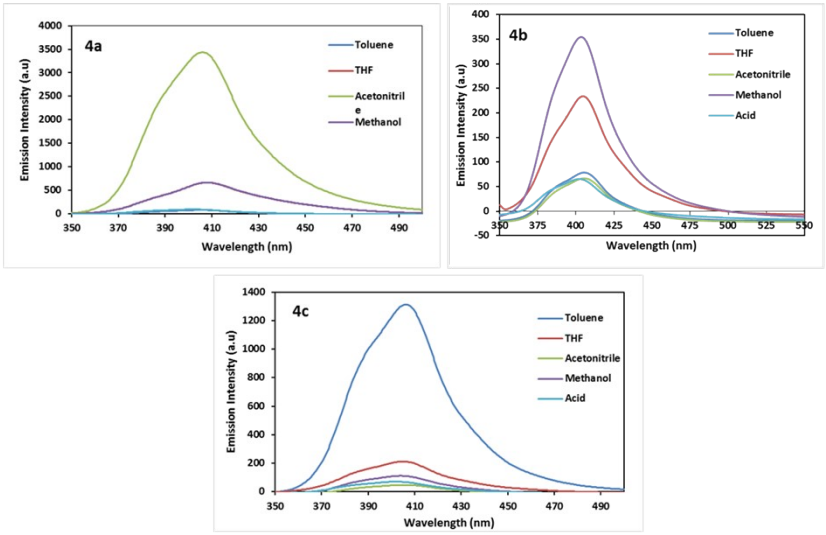

Compound	Emission Intensity(a.u)					Wavelength (nm)				
	Toluene	THF	Acetonitrile	Methanol	Acid	Toluene	THF	Acetonitrile	Methanol	Acid
4a	78.8086	662.547	3435.27	664.338	92.6087	405.5	408	406	408	402
4b	78.8086	234.224	67.0457	354.835	65.5306	405.5	404.5	405.5	408	403.5
4c	1312.27	212.328	47.681	111.818	71.0618	406	405	405	404	402

Figure S1. Fluorescence spectra of **4a, 4b,** and **4c** in toluene, THF, acetonitrile, and methanol.

DFT Calculations: Various possible geometries of molecules **4a**, **4b,** and **4c** are constructed and optimized using B3LYP/6-311+G(d,p) level of DFT. The frequency calculation is performed on the lowest energy-optimized structures to confirm the minimum on the potential energy surface. All the calculations are performed using the Gaussian 16 suite of the program.[1] The UV/Visible absorption wavelengths are calculated using TD-DFT/PBE1PBE/6-311+G(d,p) method in THF solvent. The solvent effect is considered through the polarizable continuum model (PCM).[2] The results of these

calculations are summarized in Table S1. The HOMO and LUMO and other molecular orbitals corresponding to the transitions observed of the three compounds **4a**, **4b,** and **4c** are represented in Figure S1.

Table S1: Calculated UV/Visible absorption wavelengths (λ), corresponding energies, and oscillator strengths (f) of molecules **4a**, **4b,** and **4c** using TD-DFT/ PBE1PBE/6-311+G(d,p) level of theory in THF solvent. (H is for HOMO and L is LUMO)

Compound	**λ (nm)**	**E (eV)**	**f**
4a	334.37 (H→L+2) 320.40 (H → L)	3.70 3.87	0.0127 0.0973
4b	343.16 (H-1→L+3) 314.56 (H→L)	3.61 3.94	0.0799 0.0021
4c	334.02 (H→L) 329 04 (H→L+1)	3.71 3.77	0.0130 0.0581

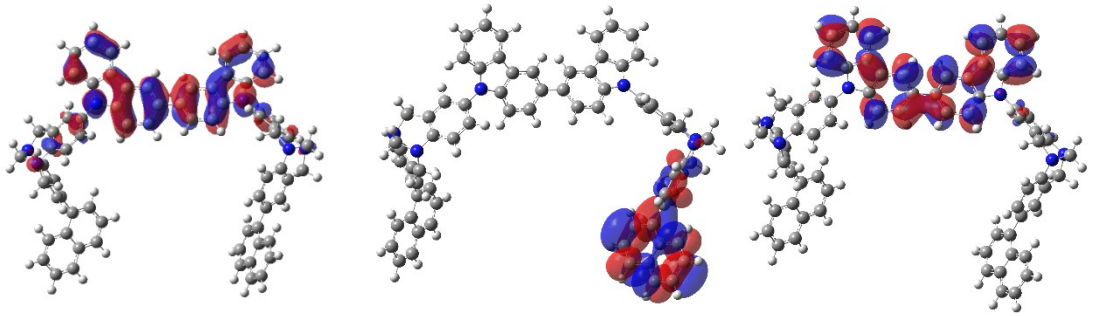

i. HOMO ii. LUMO iii. LUMO+2

Compound **4a**

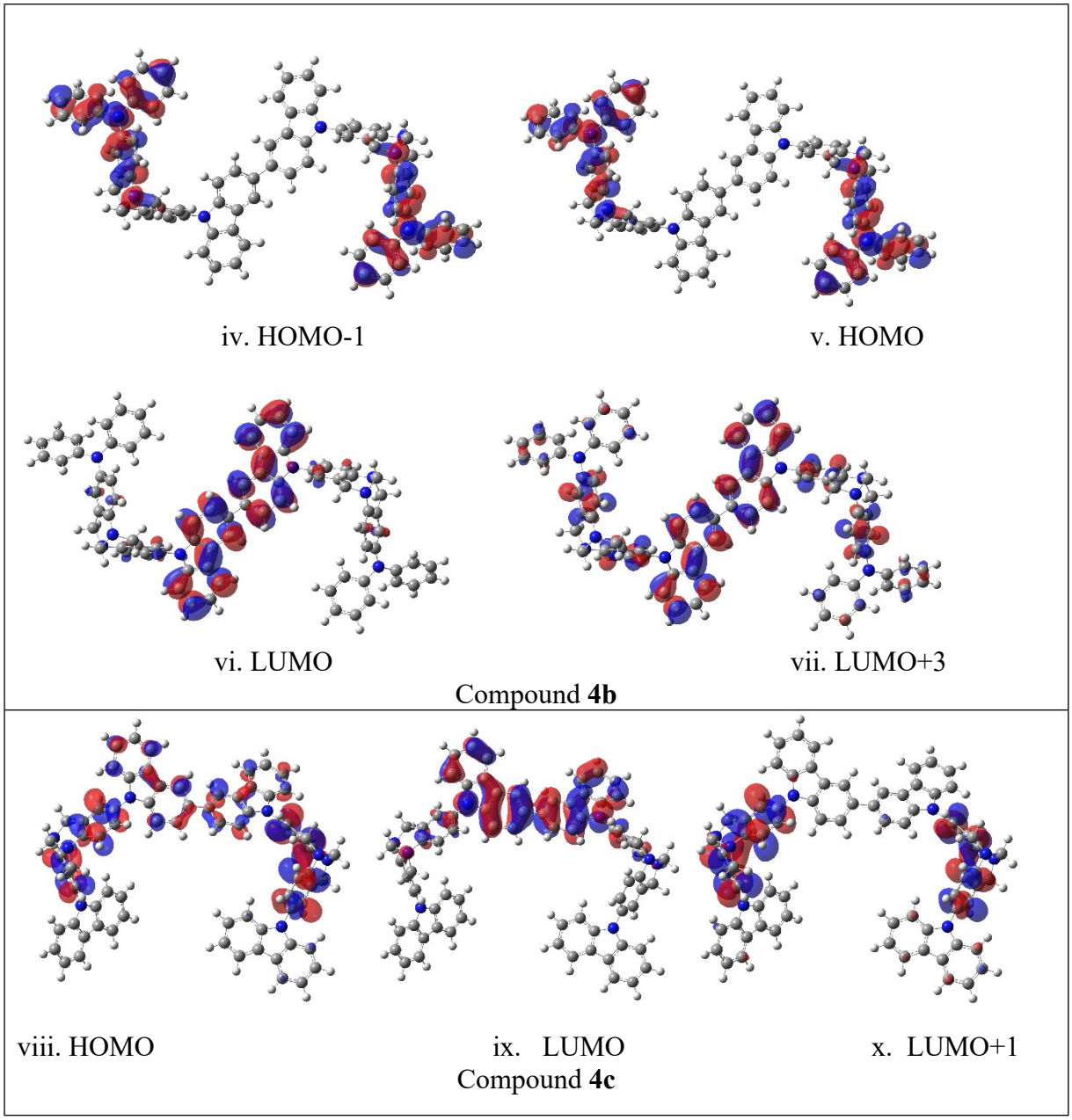

Figure S2. Molecular orbital diagrams of **4a** (i-iii), **4b** (iv-vii), and **4c** (viii-x), calculated at B3LYP/6-311+G(d,p) level of DFT, corresponding to the transitions tabulated in Table S1.

Bioimaging

Minimum inhibitory concentration (MIC) assay

MIC analysis was performed by 96 well plate broth dilution method. The activity of compounds was checked against Gram-positive (*Staphylococcus aureus* NCIM 5021) as well as a Gram-negative system (*Escherichia coli* NCIM 2045). The compound was found to not affect the survival rate of the bacterial isolates after-treatment of the drugs for 24 h. Minimum inhibitory concentration assay was performed where concentrations in the range of 2- 1024µg/ml were assessed for their effectiveness. The experiment was performed in triplicates and the standard error calculated for all the experiments were performed in triplicates [396].

$$Cell\ Viability\ (\%) = \frac{Absorbance\ of\ test\ sample}{Absorbance\ of\ negative\ control} \times 100$$

Bacterial Staining and imaging by fluorescence microscopy

A single colony of *E. coli* NCIM 2045 and *S. aureus* NCIM 5021 picked from the LB (*Luria*-Bertani) plates were incubated in LB broth overnight. After that, the bacteria were washed with 0.9% NaCl solution. The resulting bacteria with a density of 1×10^7 /mL were transferred into an EP tube and stained with **4b** (10 μM) for 10 min. Then, 10 μL of the bacteria solution was transferred onto a glass slide with a coverslip and the fluorescence images were captured using fluorescent microscope Nikon Eclipse E200. All the experiments were performed in triplicates and the standard error calculated for all the experiments was <1.

Cell viability of bacterial isolates and cancer cell lines

The compounds **4b** did not show any inhibitory action against *E. coli* as well as *S. aureus* even at the concentration of 1024μg/ml. The compounds can be said biocompatible as they are not affecting the survival of the bacterial isolates to a noticeable degree and are found to have good biocompatibility.

Table S2: Photophysical studies of 4a-4c

% Fw	Compound 4a				Compound 4b				Compound 4c			
	Experiment 1		Experiment 2		Experiment 1		Experiment 2		Experiment 1		Experiment 2	
	λex (nm)	Red region λem (nm)	λex (nm)	Red region λem (nm)	λex (nm)	Red region λem (nm)	λex (nm)	Red region λem (nm)	λex (nm)	Red region λem (nm)	λex (nm)	Red region λem (nm)
0	318	638	358	718	319	640	351	761	332	666.5	358	720
10	318	638	358	718	319	640	351	761	332	666.5	358	720
20	318	638	358	718	319	640	351	761	332	666.5	358	720
30	318	638	358	718	319	640	351	761	332	666.5	358	720
40	318	638	358	718	319	640	351	761	332	666.5	358	720
50	318	638	358	718	319	640	351	761	332	666.5	358	720
60	318	638	358	718	319	640	351	761	332	666.5	358	720
70	318	638	358	718	319	640	351	761	332	666.5	358	720
80	318	638	358	718	319	640	351	761	332	666.5	358	720
90	318	642	358	718	319	640	351	761	332	666.5	358	720
99	318	638	358	718	319	640	351	761	332	666.5	358	720

References:

[1] M. J. Frisch, G. W. Trucks, H. B. Schlegel, G. E. Scuseria, M. A. Robb, J. R. Cheeseman, G. Scalmani, V. Barone, B. Mennucci, G. A. Petersson, H. Nakatsuji, M. Caricato, X. Li, H. P. Hratchian, A. F. Izmaylov, J. Bloino, G. Zheng, J. L. Sonnenberg, M. Hada, M. Ehara, K. Toyota, R. Fukuda, J. Hasegawa, M. Ishida, T. Nakajima, Y. Honda, O. Kitao, H. Nakai, T. Vreven, J. A. Montgomery Jr., J. E. Peralta, F. Ogliaro, M. Bearpark, J. J. Heyd, E. Brothers, K.N. Kudin, V. N. Staroverov, R. Kobayashi, J. Normand, K. Raghavachari, A. Rendell, J.C. Burant, S.S. Iyengar, J. Tomasi, M. Cossi, N. Rega, J. M. Millam, M. Klene, J. E. Knox, J.B. Cross, V. Bakken, C. Adamo, J. Jaramillo, R. Gomperts, R. E. Stratmann, O. Yazyev, A. J.

Austin, R. Cammi, C. Pomelli, J. W. Ochterski, R. L. Martin, K. Morokuma, V. G. Zakrzewski, G. A. Voth, P. Salvador, J. J. Dannenberg, S. Dapprich, A. D. Daniels, O. Farkas, J. B. Foresman, J. V. Ortiz, J. Cioslowski, D. J. Fox, Gaussian 16, Revision A. 03, Gaussian, Inc., Wallingford CT, **2016**.

[2] J. Tomasi, B. Mennucci and R. Cammi, *Chem. Rev.*, 2005, **105**, 2999-3093.

^{1}H and ^{13}C NMR Spectral Reproduction of 4a-4c

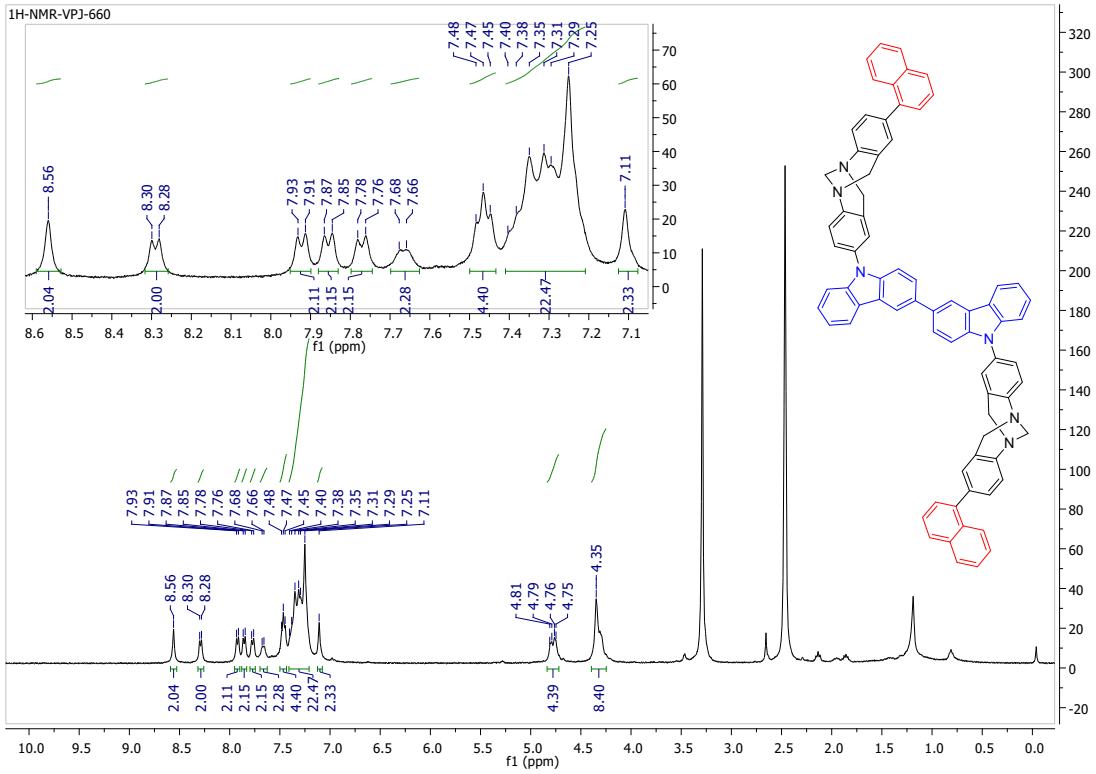

Figure S3. ^{1}H NMR (400 MHz, DMSO-d_6) of 9,9'-bis(8-(naphthalen-1-yl)-6,12-dihydro-5,11-methanodibenzo[*b*,*f*][1,5]diazocin-2-yl)-9*H*,9'*H*-3,3'-bicarbazole (**4a**).

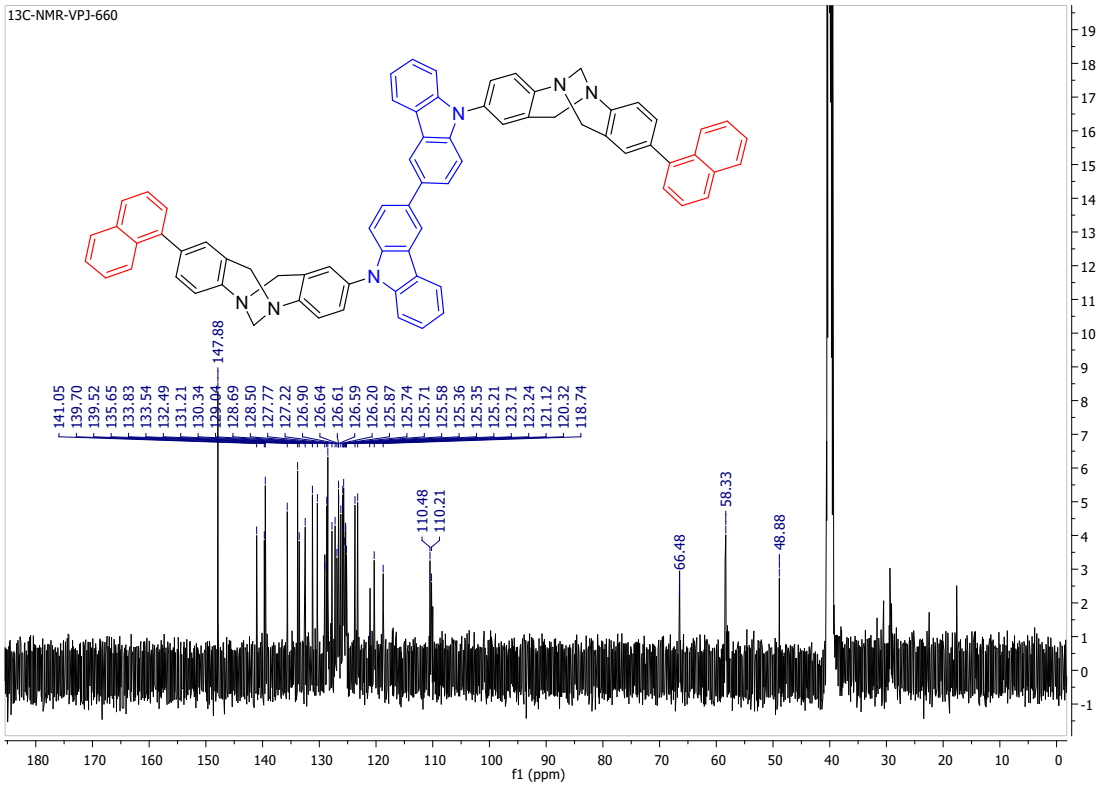

Figure S4. ^{13}C NMR (126 MHz, $CDCl_3$) of 9,9'-bis(8-(naphthalen-1-yl)-6,12-dihydro-5,11-methanodibenzo[*b*,*f*][1,5]diazocin-2-yl)-9*H*,9'*H*-3,3'-bicarbazole (**4a**).

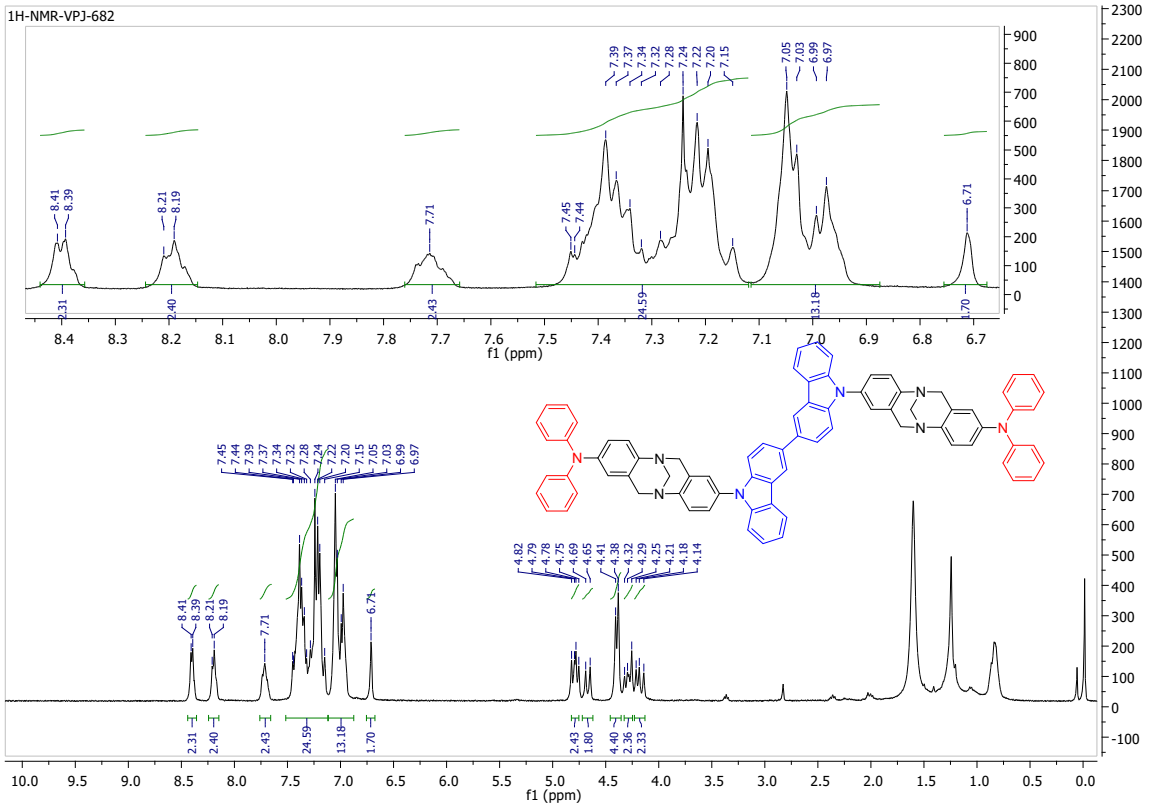

Figure S5. ^{1}H NMR (400 MHz, $CDCl_3$) of 8,8'-(9*H*,9'*H*-[3,3'-bicarbazole]-9,9'-diyl)bis(N,N-diphenyl-6,12-dihydro-5,11-methanodibenzo[*b*,*f*][1,5]diazocin-2-amine) (**4b**)

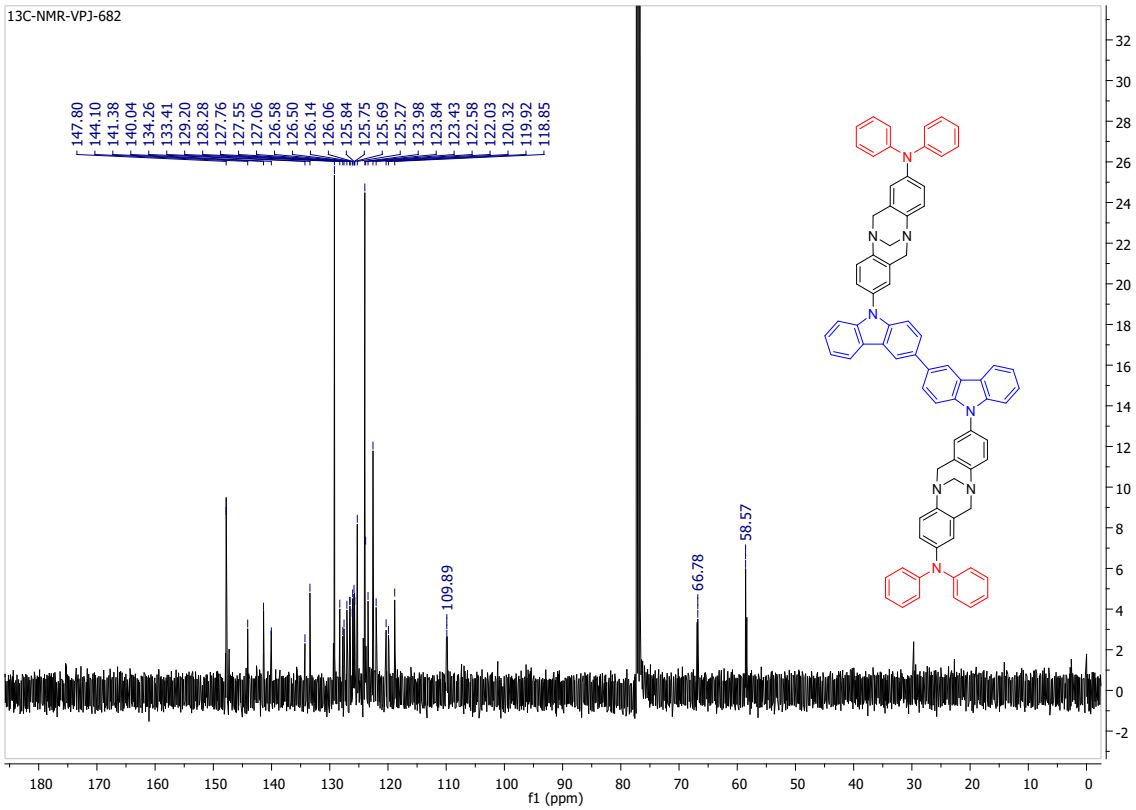

Figure S6. ^{13}C NMR (126 MHz, $CDCl_3$) of 8,8'-(9*H*,9'*H*-[3,3'-bicarbazole]-9,9'-diyl)bis(N,N-diphenyl-6,12-dihydro-5,11-methanodibenzo[*b*,*f*][1,5]diazocin-2-amine) (**4b**)

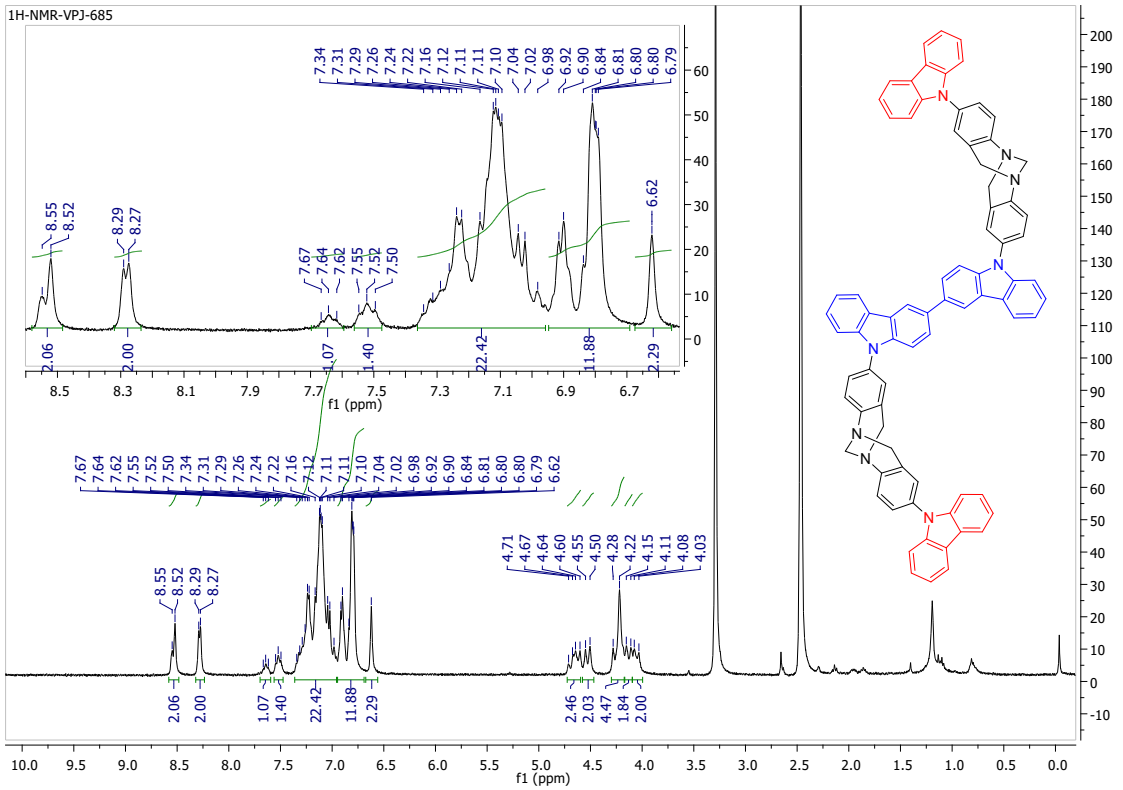

Figure S7. ^{1}H NMR (400 MHz, DMSO-d_6) of 9,9'-bis(8-(9*H*-carbazol-9-yl)-6,12-dihydro-5,11-methanodibenzo[*b*,*f*][1,5]diazocin-2-yl)-9*H*,9'*H*-3,3'-bicarbazole (**4c**).

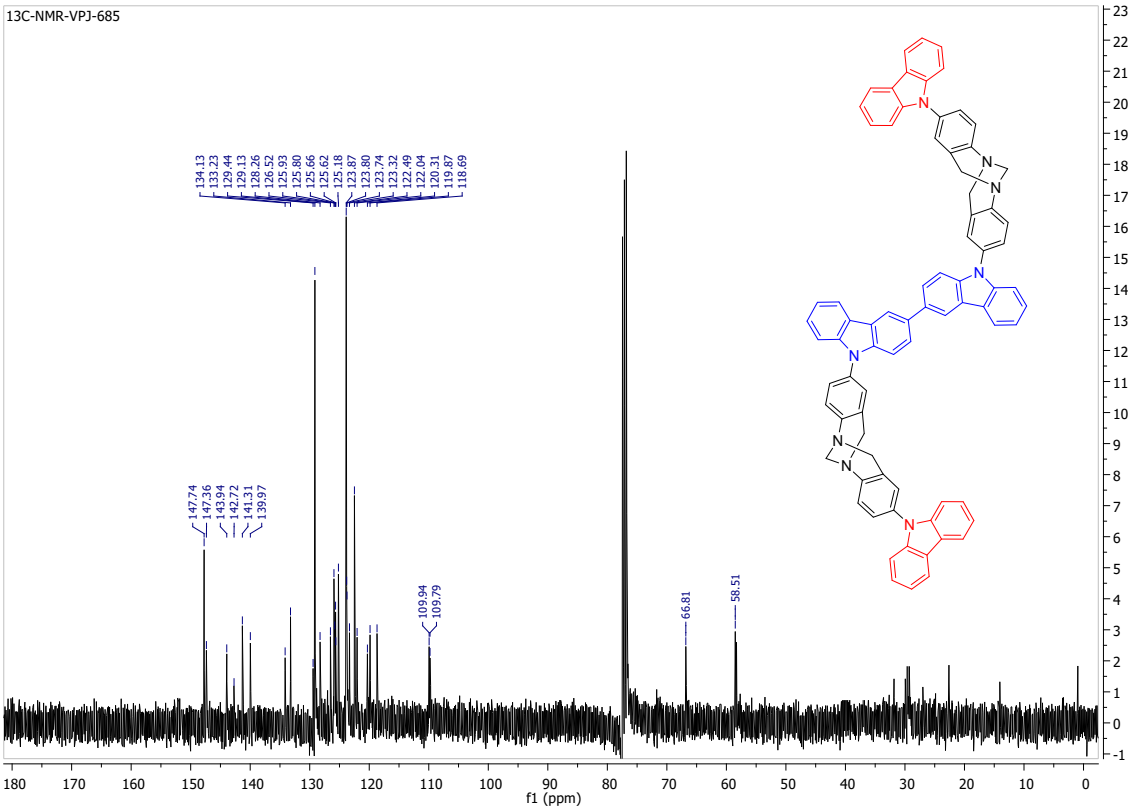

Figure S8. ^{13}C NMR (101 MHz, $CDCl_3$) of 9,9'-bis(8-(9*H*-carbazol-9-yl)-6,12-dihydro-5,11-methanodibenzo[*b*,*f*][1,5]diazocin-2-yl)-9*H*,9'*H*-3,3'-bicarbazole (**4c**).